International Journal of Mechanical Engineering and Technology (IJMET)
Volume 9, Issue 8, August 2018, pp. 253–263, Article ID: IJMET_09_08_028
Available online at http://www.iaeme.com/ijmet/issues.asp?JType=IJMET&VType=9&IType=8
ISSN Print: 0976-6340 and ISSN Online: 0976-6359

VDBA-BASED LOSSLESS AND LOSSY INDUCTANCE SIMULATORS AND ITS FILTER APPLICATIONS WITH IMPACT OF TEMPERATURE VARIATION ON RESONANT FREQUENCY AND QUALITY FACTOR OF ACTIVE GROUNDED INDUCTOR-BASED BANDPASS FILTER

Ridouane Hamdaouy* **and Khadija Slaoui**
University Sidi Mohamed Ben Abdellah, LESSI Laboratory, Department of Physics Faculty of Sciences, Dhar El Mehrez B.P. 1796, 30003 Fez-Atlas, Morocco
*Corresponding Author

ABSTRACT

This study presents a new electronically tunable active grounded inductor simulator circuit based on employing voltage differencing buffered amplifier (VDBA) as new active component. The circuit can replace spiral passive inductors for all Analog Signal Processing and data communications operations. Method/Analysis: The impact of temperature variation on its resonant frequency and quality factor are investigated using Virtuoso Analog Design Environment of Cadence @ 13-nm CMOS technology node. Findings: This paper carries out a study on CMOS realization of Voltage differencing buffered amplifier (VDBA) and its application as Bandpass Filter /High Filter circuit is realized using the VDBA based grounded inductor. Furthermore, the impact of temperature variation on the response of the bandpass filter is analyzed and presented. The performances of the proposed simulations over current mode parallel RLC and voltage mode bandpass filter circuits are shown. It is seen that the correspondence between the simulated results and the theoretical results is quite high. Novelty/Improvement: The proposed circuit uses active elements and passive elements at least two. Due to this, the circuit finds applications in all canonical operations and integrated circuit implementations.

Keywords: Active Inductor, Bandpass Filter /High Filter, Voltage differencing buffered amplifier (VDBA), CMOS technology
Cite this Article: Ridouane Hamdaouy and Khadija Slaoui, VDBA-Based Lossless and Lossy Inductance Simulators and its Filter Applications with Impact of Temperature Variation on Resonant Frequency and Quality Factor of Active Grounded Inductor-Based Bandpass Filter, International Journal of Mechanical Engineering and Technology, 9(8), 2018, pp. 253–263.
http://www.iaeme.com/IJMET/issues.asp?JType=IJMET&VType=9&IType=8

1. INTRODUCTION

Inductance is the source of many problems in electronic circuits and systems. It stands to reason that inductance radiates magnetic energy, it places a larger footprint in the integrated circuit, and it contains more parasitic noises than other components. Bulky and expensive passive inductors motivated the researchers to design the alternative circuits can be worked as inductors. Inductance simulators are widely used, especially for high frequencies, instead of inductors. Therefore, for designing filters or oscillator, for eliminating electromagnetic interferences the inductance simulators are used. Hence, realization of active inductor has become a popular research topic in research community to aid design engineer. Inductance simulations commonly used in analog signal processing applications such as active filters and oscillator circuits has an important place in the literature. Inductance simulations provide the opportunity to electronically adjust the value of the chip area used for large inductance values when compared with spiral inductances, while at the same time reducing the chip area seriously.

Thus, there are many lossless and lossy grounded inductance simulation circuits using many different active elements in the literature [1-8]. In the literature [1-4], two X-point second generation current carriers (DXCCII) based lossless and lossy inductance simulations. However, the simulations are made up of one active element and three or four passive elements. In 2005, Incekaraoglu and Çam [5] presented voltage-current based (DVCC) based series and parallel R-L inductance simulations. The building consists of one DVCC and three or four passive elements. Two first-generation current-carrying (CCI) grounded lossless and lossy inductance simulations are presented [6]. Lossless inductance simulation consists of one active element and five passive elements, but there is also a matching condition between passive elements. Operational transresistance amplifier (OTRA) based lossless and lossy inductance simulations have been proposed [7].Lossy inductance simulations come in two OTRA and five passive elements, and there is a matching requirement between passive elements in the lossless inductance simulation, which also includes six passive elements.

But these circuits suffer from one or more problems use of external passive resistors, need of some floating passive components, cannot be tuned electronically, etc.

In literature, there is VDBA or voltage dependent differential buffering (VDIBA) based active filter design and inductance simulation [8-12]. In 2014, a grounded inductance simulation with a single active element and 2 passive elements based on VDBA was presented [8]. However, the ZC-terminal is used in addition to the VDBA terminals while the structure is being constructed and the two-tier connected capacity is created. In this work, VDBA-based grounded inductance simulations are presented. The proposed structures have been realized with only one VDBA active element. Lossless inductance simulation is performed with three passive elements and there is a match condition between passive elements. Series R L and parallel R-L inductance simulations consist of only two passive elements and there is no passive element coupling condition. In addition, the capacitors used have a grounded connection. In this way, it will be less affected by the effects of parasitic impedances. Current and voltage mode filter circuits are used to demonstrate the performance of the proposed inductance simulations. Simulation and theoretical results have been shown to be in very good agreement. VLSI circuits often operate at elevated temperature due to heat generation. Moreover, the temperature of VLSI chip does not remain same throughout entire chip. Hot-spots are found to exist due to variation in activity. The circuit block which is more active gets heated and its temperature is raised generating hot-spot. Due to generation of hot-spot and variation of temperature, the circuit behavior varies. In an integrated circuit, billions

of chips exist. If the performance of chip varies, then the entire integrated circuit performs poorly. Thus this paper investigates the impact of temperature variation on circuit response when VDBA based grounded inductor for realizing bandpass filter.

2. APPLICATION OF VOLTAGE DIFFERENCING BUFFERED AMPLIFIER (VDBA) AS GROUNDED INDUCTOR

The block diagrammatic representation of the VDBA and its equivalent model are indicated in Fig.1.

Ideally, The VDBA device has high-impedance voltage differencing input terminals labeled as P and N, high impedance current output terminal Z, and low-impedance output of voltage buffer noted as W. The voltage and current characteristics can be expressed by the following matrix equation:

$$\begin{bmatrix} I_P \\ I_N \\ I_Z \\ V_W \end{bmatrix} = \begin{bmatrix} 0 & 0 & 0 & 0 \\ 0 & 0 & 0 & 0 \\ \text{gm} & -\text{gm} & 0 & 0 \\ 0 & 0 & 1 & 0 \end{bmatrix} \begin{bmatrix} V_P \\ V_N \\ V_Z \\ I_W \end{bmatrix} \quad (1)$$

With $I_Z = \text{gm}\,(V_P - V_N)$ and $V_W = V_Z$ [10].

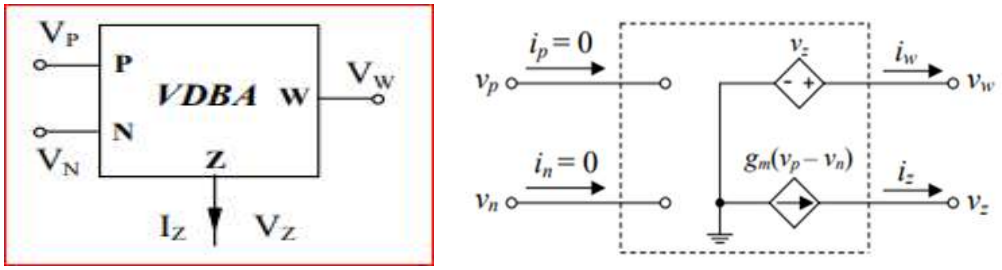

(a) **(b)**

Figure 1 Voltage differencing buffered amplifier (VDBA). (a) block diagrammatic representation,(b) equivalent model.

The parameter gm in eq.(1) refers to the transconductance gain of the VDBA, which normally is controlled by means of electronic. The internal structure of the VDBA circuit consists of two separate stages. The input stage consists of the transconductance amplifier, and the output stage consists of the buffer circuit. In this study, VDBA-based lossless and lossy inductance simulations are presented.

Fig.2 shows the proposed VDBA-based lossless inductance simulation circuit. It consists of only single VDBA, a grounded resistor and two capacitors with hence, the circuit is simple and canonical structure and very suitable for integrated circuit implementation.

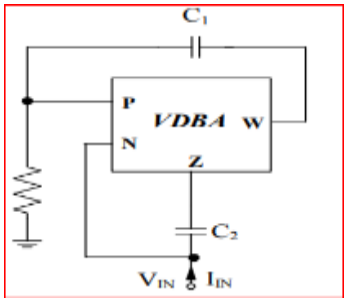

Figure 2 VDBA-based lossless inductance simulation

Routine circuit analysis yields the input impedance of the proposed grounded inductor in Fig.2 as the following expression:

$$\mathbf{Z_{in}}=\frac{\mathbf{v_n}}{\mathbf{i_n}}=\frac{\mathbf{1}}{\mathbf{g_m}}+\frac{\mathbf{SC_1}}{\mathbf{g_m}G}-\frac{\mathbf{SC_1}}{\mathbf{SC_2}G} \quad (2)$$

As can be seen from Eq. (2), in order for the inductance simulation in Fig. 2 to operate without loss, gm = G and C1 = C2 must be satisfied. The equivalent input impedance of the grounded lossless inductance simulation is

$$\mathbf{Z_{in}}=\frac{\mathbf{v_n}}{\mathbf{i_n}}=\frac{\mathbf{SC_1}}{\mathbf{g_m}G} \quad (3)$$

The sensitivity analysis of the proposed lossless inductance simulation is given in Eq. (4)

$$-\mathbf{S_G^{L_{eq}}}=\mathbf{S_{C_1}^{L_{eq}}}=-\mathbf{S_{g_m}^{L_{eq}}}=1 \quad (4)$$

The proposed second VDBA-based series R-L inductance simulation is presented in Fig3. The structure consists of a single VDBA, a grounded capacity and resistance. The transfer function of the input impedance of the structure is given in equation (5).

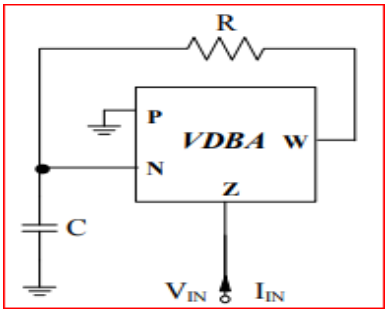

Figure 3 VDBA-based series R-L inductance simulation

$$\mathbf{Z_{in}}=\frac{\mathbf{v_n}}{\mathbf{i_n}}=\frac{\mathbf{1}}{\mathbf{g_m}}+\frac{\mathbf{SC}}{\mathbf{g_m}G} \quad (5)$$

In general, it is possible to control the gm value electronically through the external supplied current or voltage.As is evident, the inductance series resistance value is determined by the transconductance. The quality factor at the center frequency of the series R-L inductance simulation in Fig. 3 can be calculated as in equation (6). In addition, the similarity sensitivity analyzes are given in Eq. (7).

$$Q=\frac{\omega C}{\mathbf{g_m}G}*\mathbf{g_m} \quad (6)$$

$$-\mathbf{S_G^{L_{eq}}}=\mathbf{S_{C_1}^{L_{eq}}}=-\mathbf{S_{g_m}^{L_{eq}}}=1\ ,-\mathbf{S_G^{Q}}=\mathbf{S_{C_1}^{Q}}=\mathbf{S_{g_m}^{Q}}=1 \quad (7)$$

As seen from the equation, in order to increase the quality factor of the inductance simulation, it is necessary to increase the value of the transconductance used in the structure. Moreover, it is seen that passive element sensitivities do not pass unit amplitude from the analysis results.Finally, the proposed VDBA-based parallel R-L inductance simulation is shown in Fig4. Similar to the series R-L simulator, the single VDBA consists of a grounded capacity and resistance.

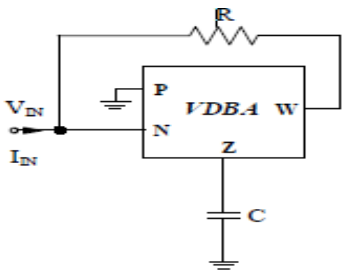

Figure 4 VDBA-based parallel R-L inductance simulation

The input transfer function of the simulant is obtained as in equation (8)

$$\mathbf{Y_{in}}=\frac{\mathbf{v_n}}{\mathbf{i_n}}=\mathbf{G}+\frac{\mathbf{g_m}G}{\mathbf{SC}} \quad 8$$

As seen from Eq. (8), the resistance parallel to the lossless inductance is determined by the external resistance used in the value structure. The quality factor of the center frequency of the simulant is given in Eq. (9).

$$Q=\frac{G}{G\omega\mathbf{C}} * \mathbf{g_m} \quad 9$$

The calculated results for the sensitivities for the parallel loss R-L simulation are given below.

$$-\mathbf{S_G^{L_{eq}}} = \mathbf{S_C^{L_{eq}}} = -\mathbf{S_{g_m}^{L_{eq}}} = 1 \ , \ -\mathbf{S_C^Q} = \mathbf{S_{g_m}^Q} = 1 \quad 10$$

3. APPLICATION OF VDBA AS GROUNDED INDUCTOR BASED ACTIVE FILTER WITH SIMULATION RESULTS

To confirm the theoretical prediction, the proposed circuit in Fig.2 was simulated with Cadence virtuoso simulations will be given to demonstrate the performance of the proposed inductance simulations. To implement the VDBA device in simulations, the TSMC13RF technology structure depicted in Fig.5 has been employed using 0.13-µm TSMC13RF.The internal structure to be used for CMOS implementation of VDBA is given in Fig. 5 [10]. Unlike the internal structure in [10], the transconductance is realized with a solid cascade current mirror in order to increase the low frequency performance of the circuit. The transistor sizes of the CMOS implementation in FIG. 5 are shown in Table 1.

The CMOS realization of the proposed VDBA with electronically and transconductance tunable is shown in Fig.5. The circuit consists of an active loaded differential amplifier M1-M2 followed by a unity-gain voltage buffer M16- M22. To improve the wide-input dynamic range of the VDBA, the transistor M1 and M2 are connected as resistance simulators. Transistor M20 introduces local negative feedback loop between node W and the drain of M16 for providing an exact voltage following and a low-output resistance at port W [13]. The equivalent small-signal terminal resistances of the CMOS VDBA shown in Fig.5 can be found as:

$$\boldsymbol{R_p}=\boldsymbol{R_n}=\infty \quad 11$$

$$\mathbf{R_z} \cong \left(\frac{\mathbf{1}}{\mathbf{g_{d2}}+\mathbf{g_{d4}}}\right) \quad 12$$

$$\mathbf{R_w} \cong \left[\frac{(\mathbf{g_{m16}}+\mathbf{g_{m17}})(\mathbf{g_{m16}}+\mathbf{g_{m18}})}{\mathbf{g_{m17}}\mathbf{g_{m16}}\mathbf{g_{m20}}}\right] \quad 13$$

Where g_{mi} and g_{di} are the transconductance and the drain conductance of the i-th transistor, respectively. To obtain the tunability for the transconductance behaviour of the VDBA, the

current biasing circuit M3-M15 of Fig.5 is employed for the current biasing circuit of differential-input transconductance amplifier M1-M2.

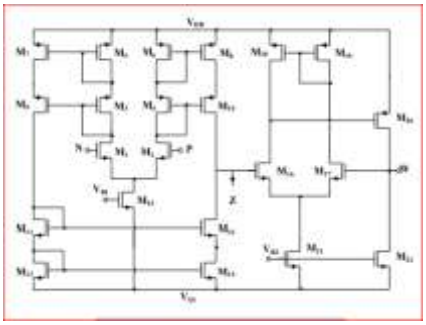

Figure 5 VDBA CMOS implementation

In this structure, the gm-value of the VDBA in Fig.5 is tunable linearly and electronically by an external DC bias of the current solid cascade current mirror.

Table 1 Transistor dimensions of VDBA CMOS implementation

Transistor	W/L (µm/µm)
M1-M6, M16,M17,M21,M22	7/0.35
M7-M10	21 /0.7
M11-M14	1 /0.7
M15	0.5 /0.35
M18-M20	14 /0.35

DC supply voltages VDD = -VSS = 3.3V, the polarity voltages are VB1 = -2.2V and VB2 = -1.7V respectively. When these values are taken, the parameters of VDBA internal structure, the parallel parasitic impedances of the Z terminal are 0.74569 MeGΩ // 40.9331 fF, the serial parasitic resistance value of the W terminal is 8.63kOhms and Power consumption is 15.407mW.In order to show the performance of the proposed inductance simulations, the variation of the inductance characteristic with frequency was examined first. Then gain-frequency responses and amplitude-time responses were investigated in different filter topologies. The ideal and simulated results of changing the impedance of the proposed inductance simulation with frequency in Fig. 2 are given in Fig6. The equivalent inductance value is obtained as 1.96mH when the capacitance and resistance value are selected as C1 = C2 = 120pF, R = 4.05k and gm = 246.913µA / V in the simulation. As can be seen, inductance simulations work like the ideal inductance between 70Hz and 11.25MHz. The parallel RLC circuit will be used to test the performance of the inductance simulation proposed in Fig2. The parallel RLC circuit implemented by the inductance simulation in Fig. 2 is shown in Fig7. The passive element values used in simulation are selected as R = 4.05kΩ , RF = 4kΩ and C1 = C2 = 120pF and CF = 100pF.

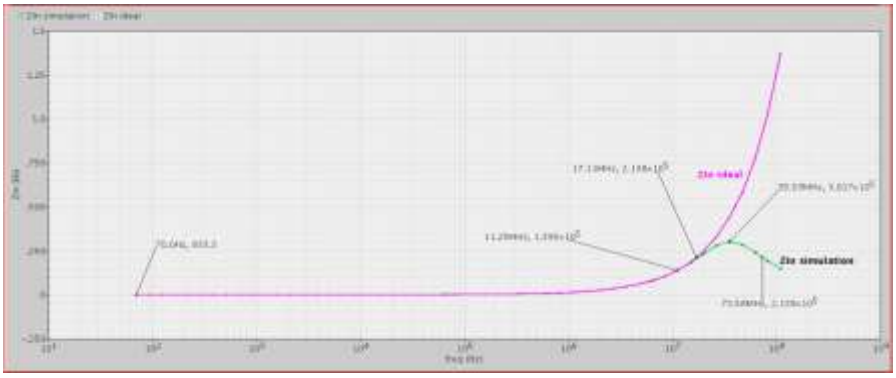

Figure 6 The impedances of the proposed simulator circuit of Fig.2 relative to frequency

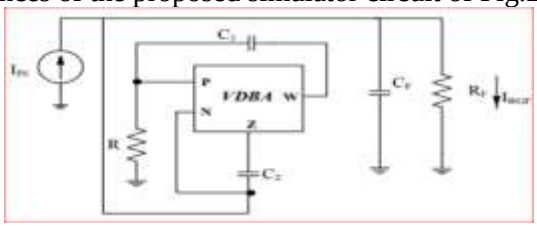

Figure 7 Parallel RLC filter

RLC filter is presented as an application example to demonstrate the performance of the presented inductance simulator. Inductance simulator with a parallel capacitor and resistor formed as a resonant circuit shown in Figure 8. In this Figure actively simulated inductance simulator circuit in Figure 2 replaces the parallel inductor.

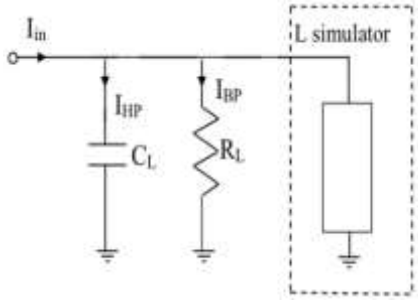

Figure 8 RLC Filter application of the proposed inductance simulator

The transfer functions are given by the following equations:

$$\frac{I_{HP}(s)}{I_{in}(s)} = \frac{S^2}{S^2+s\left(\frac{1}{R_L C_L}\right)+\frac{1}{L_{eq}C_L}} \quad \text{with} \quad C_L = C_F \quad \text{and } R_L = R_F \tag{14}$$

$$\frac{I_{BP}(s)}{I_{in}(s)} = \frac{\left(\frac{1}{R_L C_L}\right)S}{S^2+s\left(\frac{1}{R_L C_L}\right)+\frac{1}{L_{eq}C_L}} \quad \text{with} \quad C_L = C_F \quad \text{and } R_L = R_F \tag{15}$$

$$f_0 = \frac{1}{2\pi}\frac{1}{\sqrt{L_{eq}C_L}} \tag{16}$$

$$Q = \frac{R_L C_L}{\sqrt{L_{eq}C_L}} \tag{17}$$

The gain frequency response of the current mode highpass and bandpass filters is given in Figure 9. The center frequency and quality factor of the bandpass filter wer336.8 KHz and 0.85, respectively. For the center frequency and quality factor, the margin of error between

the simulated and ideal results is 26.91% and 38.86%, respectively. The causes of the difference are the parasitic impedances of the active element.

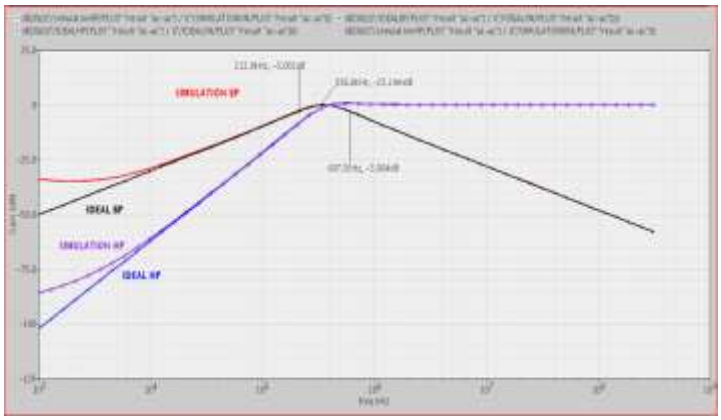

Figure 9 Ideal and simulated of the gain frequency response of the current-mode filter circuit of Fig.7

For this filter, there is small deviation between ideal and simulated responses in the low-frequency region of the frequency response. The frequency responses of the filter in Fig. 7 are shown in Fig.9. It appears, thus, that the simulated and ideal values are in good agreement. In addition, the amplitude-time response of the bandpass filter output is shown in Fig10. The total harmonic distortion (THD) is 73.57% when 106.84µA peak-to-peak amplitude 1MHz sinus signal is applied to the filter circuit of Fig7.To demonstrate the performance of the parallel inductance simulation in Fig. 4, the voltage mode bandpass filter topology given in Fig.11 is used. As you can see, the external load resistor is not connected. Instead of the load resistance, the parallel resistor in the proposed topology is used.

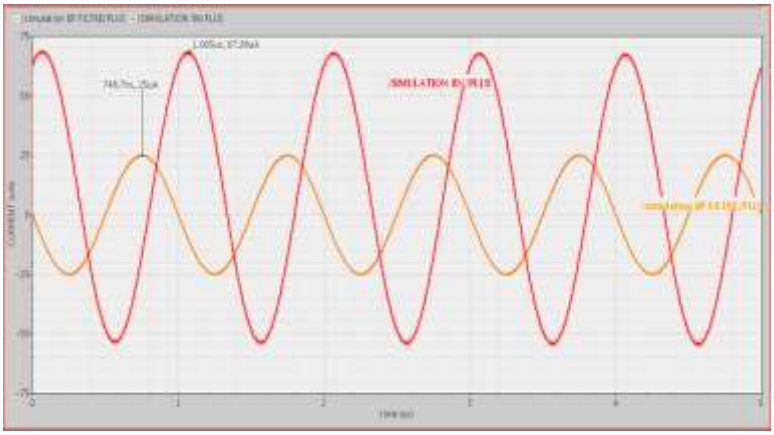

Figure 10 Time domain response of current-mode bandpass filter output

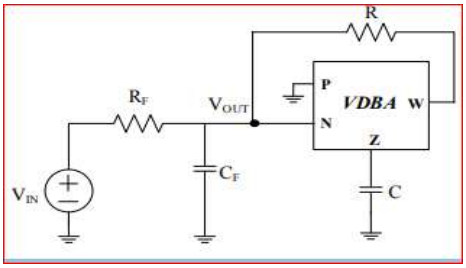

Figure 11 Voltage-mode bandpass filter circuit

For the simulation, passive element values R = 4.05kΩ, RF = 4kΩ , C = 120pF and CF =100pF are selected for the center frequency f0 = 337kHz and the quality factor Q = 0.4284. The gain frequency response of the voltage mode bandpass filter circuit is given in Fig12. For the center frequency and quality factor, the margin of error between the simulated and ideal results is 1.05% and 0.168%, respectively.The amplitude-time response of the voltage-mode bandpass filter output is given in Fig13. The total harmonic distortion (THD) is 0.015% when a 1MHz sinus signal of 189.92mV peak-to-peak amplitude is applied to the input of the voltage mode bandpass filter circuit in Fig11.

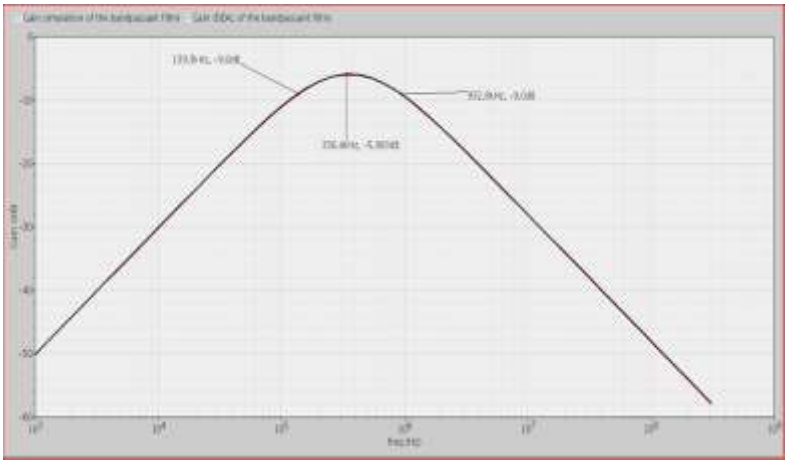

Figure 12 The gain-frequency response of the voltage-mode bandpass filter circuit

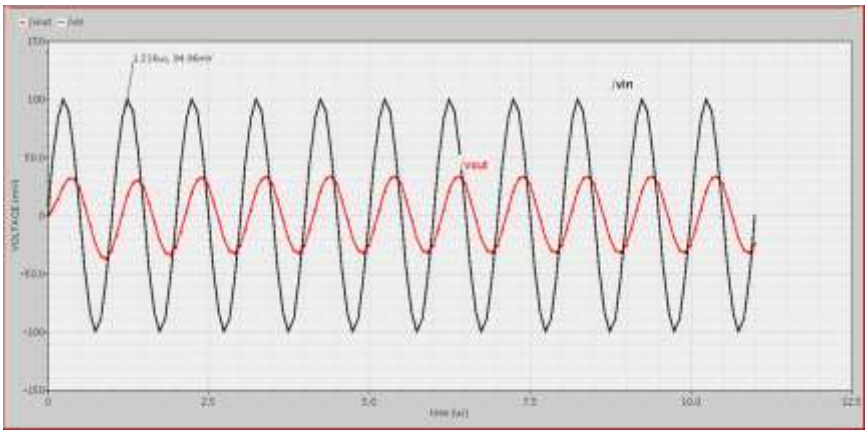

Figure 13 Time domain responses of voltage-mode bandpass filter output.

Note: Computer simulation results are performed to verify the workability of the designed simulator circuit and its application.

4. IMPACT OF TEMPERATURE VARIATION ON RESONANT FREQUENCY AND QUALITY FACTOR OF VOLTAGE-MODE BANDPASS FILTER CIRCUIT

This section presents the AC analysis of bandpass filter in figure 11 which is designed using grounded inductor. The grounded inductor in turn is realized employing voltage differencing buffer amplifer (VDBA). The analysis is carried out at different temperatures .The carrier mobility μ_n and the threshold voltage $V_T$decrease with temperature. Temperature dependence of $V_T$is expressed as

$$\boldsymbol{V_T(T)=V_T(T_0)+\alpha_{V_T}(T-T_0)} \quad 18$$

Where T_0 is the reference temperature and α_{V_T} is a negative constant.

Temperature dependence of mobility is given by

$$\mu_n(T)=\mu_n(T_0)(T/T_0)^{\alpha_\mu} \quad 19$$

It is observed that the effect of decrease in mobility with temperature dominates and thus the transconductance of a MOSFET decreases with increase in temperature [14].To verify the temperature dependence of resonant frequency (fr) and quality factor(Q) of the bandpass filter circuit, extensive simulations on Virtuoso Analog Design Environment of Cadence using 13-nm Technology Model are performed. The response of the bandpass filter in figure 11 is analyzed at two different temperatures to observe the departure of resonant frequency and quality factor from the theoretical values. They are 27°C (room temperature), 109°C and 191°C shown in Figure 14. The simulation results are tabulated in Table 2. It is observed that the resonant frequency and quality factor shifts towards lower frequencies and lower quality factor as the temperature increases. This is attributed to the fact that the transconductance of a MOSFET decreases with increase in temperature due to the dominant effect of mobility.

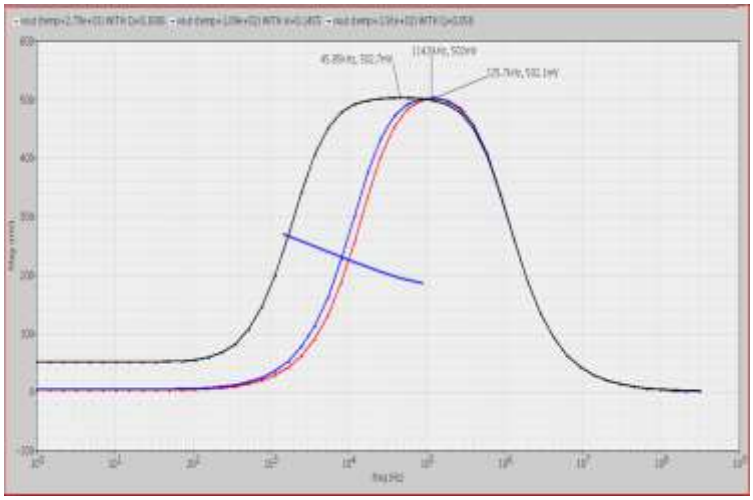

Figure 14 Variation of resonant frequency (fr) and Quality factor(Q) of Bandpass Filter with temperature. The graph shows decrease of resonant frequency and quality factor with increase in temperature. It shows fr = 125.7 kHz and Q=0.1606@ 27°C, fr = 114.5 kHz and Q= 0.1455@ 109°C and fr = 45.85kHz and Q=0.058@ 191°C.

Table 2 The simulation results.

Temperature(in °C)	27	109	191
Resonant Frequency(in KHz)	125.7	114.5	45.85
Quality factor(Q)	0.1606	0.1455	0.058

5. CONCLUSION

An electronically-controllable active grounded inductor circuit was designed based on the Voltage differencing buffered amplifier (VDBA) configuration using Virtuoso Analog Design Environment of Cadence. In this study, three different grounded inductance simulations with VDBA base are presented. Advisable inductance simulation circuits, lossless inductance simulation, series and parallel loss inductance simulations. Equations related to the transfer functions, quality factors and sensitivities of the proposed inductance simulations are given. Temperature variability analysis was performed to observe the temperature dependence of

resonant frequency and quality factor of the Voltage-mode bandpass filter circuit designed using VDBA based active grounded inductor.The performances of the proposed simulations over current mode parallel RLC and voltage mode bandpass filter circuits are shown. It is seen that the correspondence between the simulated results and the theoretical results is quite high.The resonant frequency and quality factor of the active grounded inductor can be electronically tuned.At higher frequencies, the active inductor is subjected to various parasitic effects.The active inductor circuit finds its application in high-speed analog signal processing and data communication systems.

REFERENCES

[1] Kacar, F., Yesil, A. Novel grounded parallel inductance simulators realization using a minimum number of active and passive components. Microelectronics Journal, 41(10), 632 638, 2010

[2] Myderrizi, I., Minaei, S., Yuce, E. DXCCII-based grounded inductance simulators and filter applications. Microelectronics Journal, 42(9), 1074-1081, 2011

[3] Yesil, A., Kacar, F. New DXCCII-based grounded series inductance simulator topologies. IU-Journal of Electrical & Electronics Engineering, 14(2), 1785-1789, 2014.

[4] Metin, B. Supplementary inductance simulator topologies employing single DXCCII. Radioengineering, 20(3), 614-618, 2011.

[5] Incekaraoglu, M., Cam, U. Realization of series and parallel RL and CD impedances using single differential voltage current conveyor. Analog Integrated Circuits and Signal Processing, 43(1), 101-104, 2005

[6] Arslan, E., Metin, B., Herencsar, N., Koton, J., Morgul, A., Cicekoglu, O. High performance wideband CMOS CCI and its application in inductance simulator design. Advances in Electrical and Computer Engineering, 12(3), 21-26, 2012

[7] Cam, U., Kacar, F., Cicekoglu, O., Kuntman, H., Kuntman, A. Novel two OTRA-based grounded immitance simulator topologies. Analog Integrated Circuits and Signal Processing, 39(2), 169-175, 2004.

[8] Yesil, A., Kacar, F., Gurkan, K. Lossless grounded inductance simulator employing single VDBA and its experimental band-pass filter application. Int. J. Electron. Commun. (AEÜ), 68, 73– 78, 2014

[9] Khatib, N., Biolek, D. New voltage mode universal filter based on promising structure of voltage differencing buffered amplifier. In Radioelektronika (RADIOELEKTRONIKA), 2013 23rd International Conference (pp. 177-181). IEEE.

[10] Kacar, F., Yesil, A., Noori, A. New CMOS realization of voltage differencing buffered amplifier and its biquad filter applications .Radioengineering, 21(1) 333-339, 2012

[11] Herencsar, N., Cicekoglu, O., Sotner, R., Koton, J., Vrba, K. New resistorless tunable voltage-mode universal filter using single VDIBA. Analog Integrated Circuits and Signal Processing, 76(2), 251-260, 2013.

[12] Biolek, D., Biolkova, V. First-order voltage-mode all-pass filter employing one active element and one grounded capacitor. Analog Integrated Circuits and Signal Processing, 65(1), 123-129, 2010.

[13] W. Surakampontorn, V. Riewruja, K. Kumwachara, and K. Dejhan, “Accurate CMOS based Current Conveyors”, IEEE Trans. Instru. Meas., vol.40, no.4, pp. 699-702, 1991.

[14] Filanovsky IM, Allam A. Mutual compensation of mobility and threshold voltage temperature effects with applications in CMOS circuits. IEEE Transactions on Circuits and Systems - 1: Fundamental Theory and Applications. 2001 Jul; 48(7):876–84.